

A comparative study of different statistical methods for Flood susceptibility assessment: A case study of N'fis basin, Marrakesh High Atlas (Morocco)

Hassan Ait Naceur^{1*}, Ibrahim Igmoulan¹, Mustapha Namous², Omar Bourouy¹ and Mustapha Ouayah²

1. Laboratory of Laboratory of Georesources, Geoenvironment and Civil Engineering (L3G), Faculty of Sciences and Technology, Cadi Ayyad University, Marrakesh, MOROCCO

2. Laboratory of Biotechnology and Sustainable Development of Natural Resources, Polydisciplinary Faculty, Sultan Moulay Slimane University, Mghila B.P. 592, Beni Mellal, MOROCCO

*Hassan.aitnaceur@ced.uca.ma; Hsnggeo@gmail.com

Abstract

Floods are one of the natural disasters with far-reaching socio-economic and environmental consequences. A large part of the N'fis catchment area is vulnerable to the risk of flooding which causes an immense loss of people and infrastructure. Therefore, an accurate assessment for the susceptibility of natural risks remains essential. The main objective of this study is to evaluate the performance of frequency ratio (FR), informative value (IV) and weight of evidence (WoE) models in flood sensitivity mapping in the N'fis watershed, high atlas of Marrakech in central Morocco. A total of 87 paleo-floods sites were inventoried based on data from Tensift hydraulic agency and extensive field surveys and 11 causative factors were considered in this study.

The results show high susceptibility in the northern part of the N'fis basin and moderate to low susceptibility in its southern parts. The maps were validated according to the receiver operating characteristic (ROC) curve and the area under the curves (AUC) was calculated. Then, the accuracy rates are of the order of 85.65%, 87.75% and 88.40% for the FR, IV and WoE models respectively. Thus, the WoE model proved to be the most significant model for the analysis of flood sensitivity in this region. The results of this work can be an important support for decision-makers for flood risk-appropriate planning.

Keywords: Flood risk, Frequency ratio, Informative value, Weights of Evidence, GIS, N'fis catchment.

Introduction

Flooding is the temporary submersion of land by water that is not normally submerged. It is considered to be one of the major natural hazards in the world that can cause loss of human life, damage to infrastructure, environmental degradation and displacement of people. On average, floods affect 140 million people³⁹ with 20,000 victims each year.⁴¹

In the Mediterranean region, the scale of ancient floods and the increase in their frequency require local planners and

***Author for Correspondence**

decision-makers to take the flood risk into consideration more and more. In this context, the identification of the areas likely to be affected by floods is essential for a better management of this risk.³⁶

Morocco experienced major floods at the beginning of the 21st century that caused significant economic damage in several regions of the country for example, the catastrophic events of the Ourika Valley in 1995, the city of Tetouan and the plain of Martil in 2000, the regions of Mohammadia, Berrechid and Settat in 2002, the region of Tangier in 2008, the plain of Gharb in 2009, the region of Taza in 2010 and the region of Khenifra in 2011.

The development of a flood sensitivity map for prone areas is an important task for the infrastructure protection. It can also provide an essential basis for emergency services when implementing management strategies to prevent and mitigate future flood events.

Recently, the development of GIS tools and the availability of remote sensing data sources has greatly facilitated the construction and execution of predictive models for areas sensitive to natural hazards. However, conventional flood modelling methods were not reliable for accurate prediction.⁴⁵ Currently, geo-spatial techniques provide a wide range of data sources for good quality flood modelling.⁴⁹ Some of the most widely used models include: (AHP) "Analytical Hierarchy Processes", Weights of Evidence (WoE),³³ Logistic Regression (LR),^{33,34} Adaptive Neuro-Flooding. Artificial neural networks (ANN)³¹ and the Frequency Ratio FR model.^{20,22,34}

The main objectives of this research are: (1) Production of flood risk vulnerability maps in the N'fis catchment area by using three models, namely: Frequency Ratio (FR), Weights of Evidence (WOE) and Informative Value Method (IV). (2) Evaluation and comparison of the prediction performance of these three models in a mountain environment with a semi-arid climate and (3) Identification and ranking of the importance of the floods causative factors.

The accuracy and predictive quality of the resulting maps is evaluated with reference to the Receiver Operating Characteristic (ROC) method and the Area under Curve (AUC) calculation.

Study area

The basin of N'fis is located southwest of Marrakech city. It is one of the most important watersheds of the Western High Atlas of Morocco. The basin is oriented NE-SW between latitudes 30.5 and 31.2°N and longitudes 7. 55° and 8. 40°W with an area of about 1712 Km². The altitude of the basin varies from 669 to 4143 m above sea level with an average altitude and slope of 1864 m and 23° respectively.

Geomorphologically, this basin is a part of the high atlas of Marrakech. It is characterized by rugged relief with altitudes ranging from 669 to 4146 meters. The slopes are very steep with escarpments and cliffs within the Cambrian carbonate formations in Ijoukak area especially, where the rivers incisions develop very deep gorges formation. These slopes are marked by the formation of quaternary superficial deposits of dominated by alluvial cones, fluvial and torrential terraces whose surfaces are eroded by channels more or less deep.²⁸

In the geological setting, the N'fis basin is essentially formed by a basement affected by Hercynian orogeny surmounted by a secondary and tertiary age cover. Its upstream part,

located in the axial zone of the High Atlas, is formed by magmatic terrains (granites, granodiorites andesites, rhyolites and basalts) and metamorphic rocks (schists, gneiss and quartzites). The downstream part is represented by plateau areas constituted by mesozoic and cenozoic terrains with an alternation of softer rocks: sandstone, siltstone and clay (Fig. 1). All these geological formations are highly structured and traversed by a network of faults and fractures.³

The climate in the N'fis basin is semi-arid.² Precipitation shows spatial and temporal variability with annual averages of the order of 375 mm yr⁻¹. This precipitation is more important in the southern and southeastern regions characterized by a higher relief. Temporally, high monthly precipitation is recorded in March and April while minimum values are measured in July and August. Two main seasons can then be distinguished: a wet season from October to April where almost all rainy episodes occur with an average of 84% of annual rainfall and a dry season from May to September with only 16% of annual rainfall on average. The annual temperature is about 18.6°C with a maximum of 47.5°C in July and a minimum of -7.5°C in January.

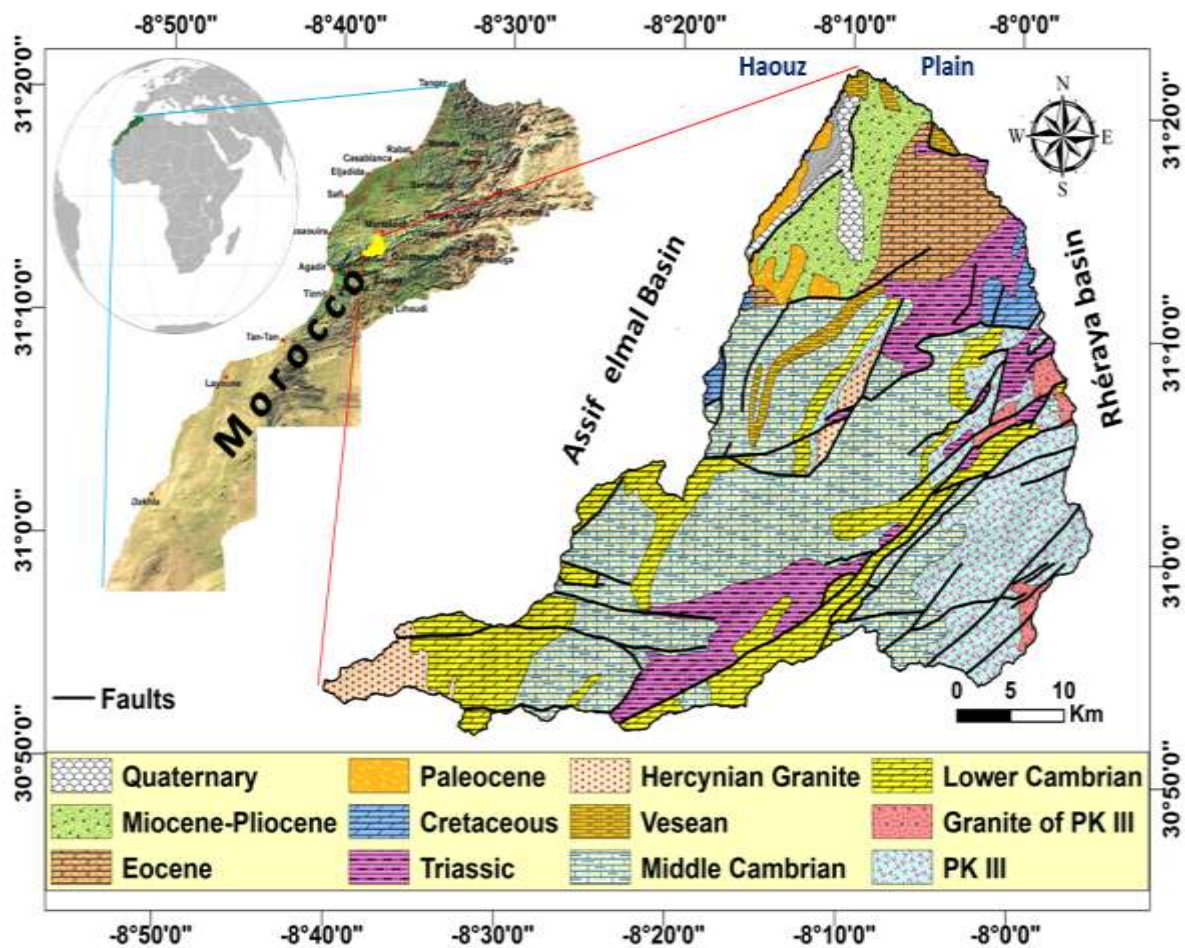


Fig. 1: Geographical location of the N'fis catchment area

Material and Methods

The present research adopts a methodology based on four steps: (1) identifying the ancient flood locations in the study area and creation of the flood inventory map. (2) choosing and classify the flood-related factors with an attached map for each variable based on the available data sources. (3) producing the flood sensitivity maps by applying the three models FR, IV and WoE and (4) validation of the results by the ROC/AUC methods and by the field survey missions with verification and assimilation by comparing to GIS. Figure 2 shows the flowchart of the methodology adopted.

Flood inventory: The first step is devoted to locating the ancient floods sites. This is an important step to analyse the correlation between flood occurrences and conditioning factors, since the ancient flood location and identification have very important impact on the accuracy and production of the flood sensitivity map of an area.²⁵

The flood inventory map was produced by field survey data as well as the treatment and the interpretation of google earth satellite images which allows us to determine the spatial

distribution of ancient flood sites in the N'fis catchment area. A total of 87 paleo-floods sites were recorded whose spatial distribution is illustrated by an inventory map, a method that has been adopted in several studies.^{4,8,13,38}

Subsequently the data from this inventory were randomly subdivided into a training and testing data, about 70% was used for model training and the remaining 30% was used to evaluate the accuracy and predictive quality of the developed models. The map in the figure 3 shows the flood locations used in this research.

Flood conditioning factors: The second stage is consecrated to the selection and reclassification of flood-related sub-factors. There are no conditions limits for imposing exactly which set of variables a model should contain. However, most studies evaluate the geological and geomorphological variables as the important conditional factors.^{42,44} In our case, eleven factors were analysed: lithology, land use, elevation, slope angle, aspect, topographic moisture index (TWI), profile curvature and distance to river, precipitation, soil type and NDVI.

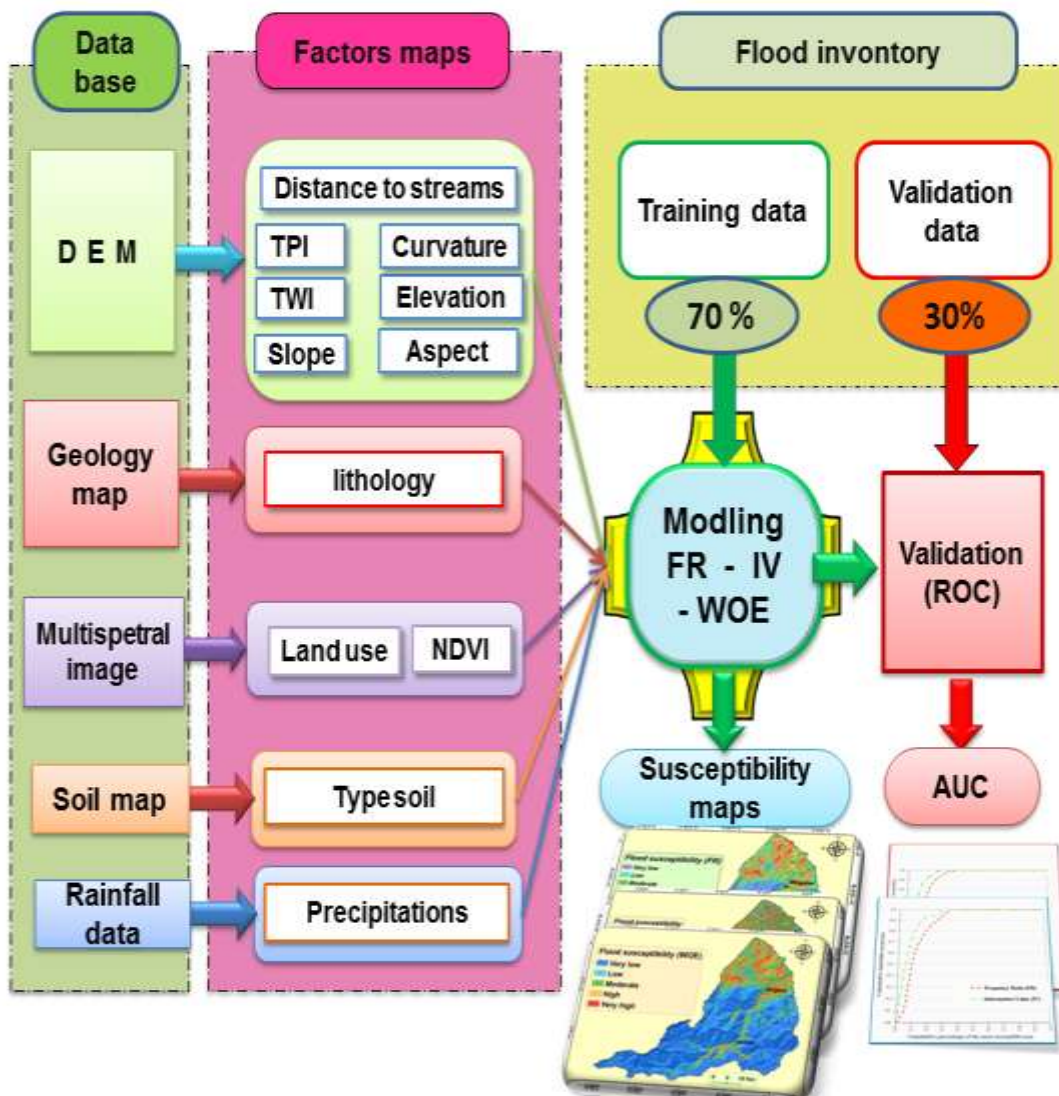


Fig. 2: Flow chart of the developed methodology

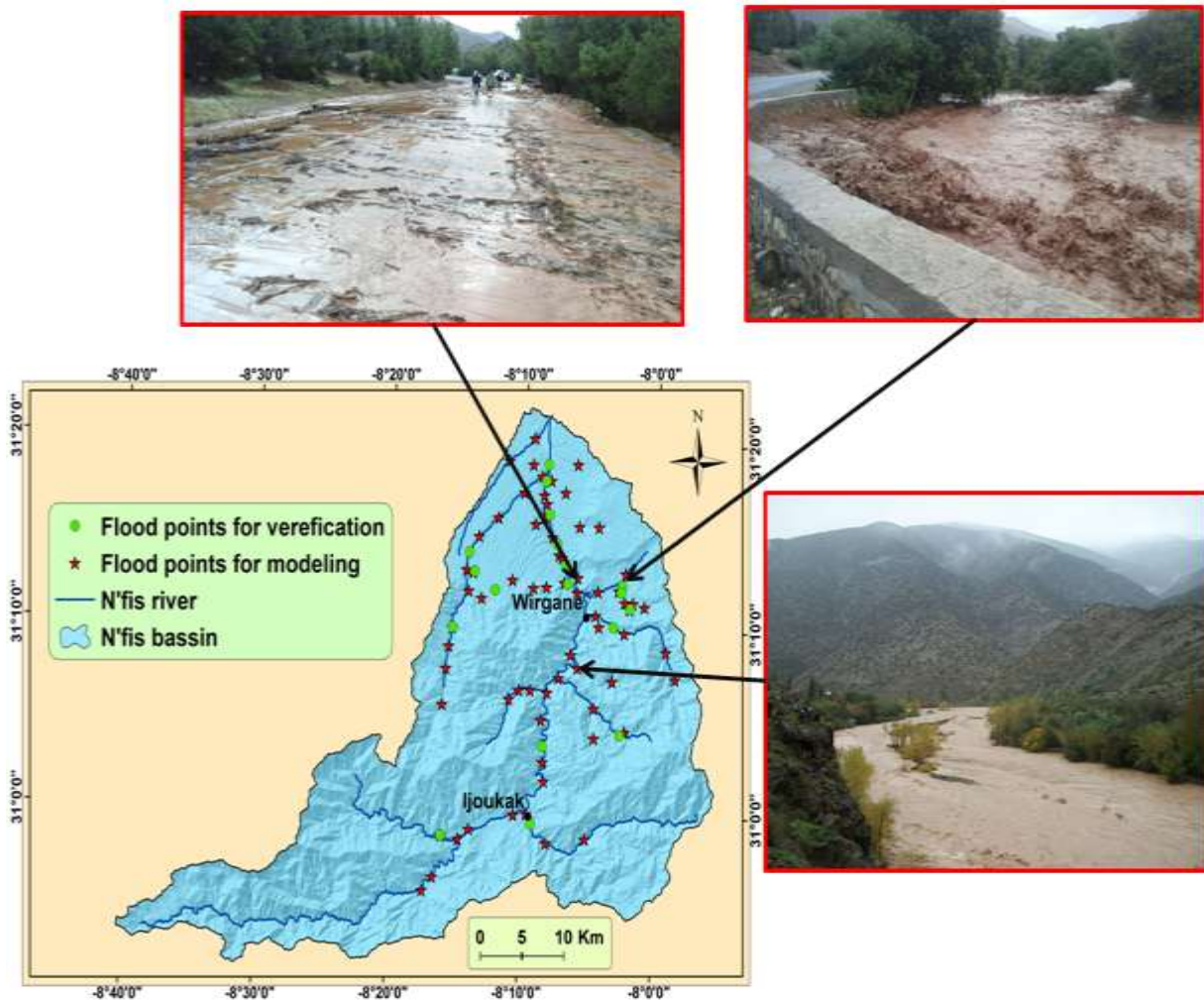


Fig. 3: Inventory map and examples of flood in the N'fis watershed area

According to Miller et al,²⁶ lithology is a key factor responsible for the spatiotemporal variation observed in hydrology and sediment production in a watershed which plays a very important factor influencing and increasing the flooding occurrence probability.³⁷ In our case, the geological map of Morocco (1/1000 000) is to produce the lithological map of N'fis river catchment (fig. 4A). Several morphometric parameters of the study area were extracted from the digital elevation model (DEM) downloaded from the <https://search.asf.alaska.edu> website with a resolution of 12.5 m. The slope angle and elevation are inversely proportional to the occurrence of flooding and considered as an important parameter in forecasting areas likely to be flooded.^{19,31} Generally steep slope area produces and increases flow velocity which results in the occurrence of flash floods in flat zones.

The altitudes map of the N'fis watershed has been subdivided into nine elevation classes (669-1000) (1000-1400) (1400-1800) (1800-2200) (2200-2600) (2600-3000) (3000-3400) (3400-3800) (3800-4146 m) (Fig.4B) while the slope map was reclassified into five classes (Fig.4C): (0°-5), (5-10), (10-15), (15-20), (20-25), (25-30), (30-35), (35-40), (40°<). Also, for aspect factor which can affect the hydrological

conditions since it is related to soil moisture patterns and physiographic trends,¹⁴ the slope aspect map produced from the DEM was classified into nine classes, eight flanks with a slope direction and one flat class (Fig. 4D).

Topographic Moisture Index (TWI), which reflects the effect of topography on the distribution of soil moisture in an area, is considered to be an index that can predict areas to be saturated and to produce runoff. A high TWI value indicates that the land is more water saturated and this automatically led to the occurrence of a flash flood.¹¹

Figure 4E shows the TWI map for the N'fis watershed reclassified into six classes (1.2-2.4), (2.4-5), (5-5.75), (5.75-6.5), (6.5-8.5) and (8.5-24.2).

Rainfall is one of the most reliable factors in floods forecasting techniques and we cannot imagine a flood phenomenon without the influence of that factor.¹¹ The rainfall data used in this study were provided by the Water and Forestry department and the Tensift River Basin Agency (ABHT). The splint interpolation technique was used to estimate a rainfall map for the area with eight classes subdivisions: (230 mm-300), (300-350), (350-400), (400-

450), (450-500), (500-550), (550-600) and (600-630) (fig.4F).

Vegetation is a protective factor which decreases the probability of flooding because it acts as a natural obstacle and decreases the flow velocity. Thus, for estimating the vegetation density, NDVI is the most efficient and reliable index. The NDVI map was prepared from Sentinel 2A images using equation (1) and reclassified into six subclasses: (-1 - 0), (0 - 0.2), (0.2 - 0.3), (0.3 - 0.4), (0.4 - 0.5), (0.5 - 0.7), (0.7 - 1) (Fig. 4G):

$$NDVI = \frac{(PIR-R)}{(PIR+R)}$$

Generally, in a catchment area, sites close to rivers are more prone to flooding. So the factor called distance from the river is the most important factor influencing flooding and it leads to threat damage because proprietaries are widely used in flood sensitivity analyses.^{32,39,47} The extent and magnitude of floods depend on the distance from the river or river channel. In the present study, seven classes using buffer tool zones were developed at a distance of 100 m from the center of river (fig. 4H).

Surface curvature refers to the rate of change of slope in a particular direction.⁴⁸ Curvature influences erosion processes on hills slopes through the convergence and divergence of flows.¹⁴ Negative and positive curvature values represent concave and convex surfaces while the zero-curvature value represent a flat surface (Fig. 4I).

Land use types affect the degree and frequency of flooding in an area.^{5,15} Each land use category has a specific influence degree on the occurrence of flood risk⁴³. Infiltration and runoff depend on land use type and other factors. Changes in land cover due to anthropogenic activities such as urbanization, deforestation and cultivation lead to an increase in the frequency and severity of floods risk. In N'fis watershed, the land-use map was obtained by processing satellite images coupled with aerial photographs (supervised multi-spectral classification) which were validated by referring to observations collected from field missions (fig. 4J). The N'fis catchment area shows areas of bare soil with less vegetation cover and other rocky outcrops. On the other hand, there are areas with low to medium vegetation cover and areas with dense vegetation which occupy small percentage in the catchment.

Soil factor affects infiltration and runoff and therefore have a significant impact on floods risk management. For example, in our study case, soils rich in clay are mostly impermeable and cause more runoff which will lead to flooding of the region. The soil map was developed from Mathieu²⁴ (fig. 4k).

Methodology

Frequency Ratio: Several research studies have adopted the frequency ratio method in predicting the susceptibility to

flooding in various regions of the world. A simple geospatial assessment tool for understanding the probabilistic relationship between dependent and independent variables including spatial data sets with multiple classification levels can be applied to the FR model.

This approach can be described as an FR index that represents the quantitative relationship between the occurrence of flash flood hazards and various conditioning parameters. It is expressed on the basis of equation (1):

$$FFHSI = Fr1 + Fr2 + Fr3 + Fr4 \dots \quad (1)$$

where FFHSI is the flash flood hazard susceptibility index and FR is the frequency ratio for each parameter. The FR can be defined as the ratio of the area where flash flooding hazards may occur to the total study area, or the ratio of the probability of a flash flood hazard occurrence to a non-occurrence as shown in equation (2):

$$FR = \frac{A/B}{M/N} \quad (2)$$

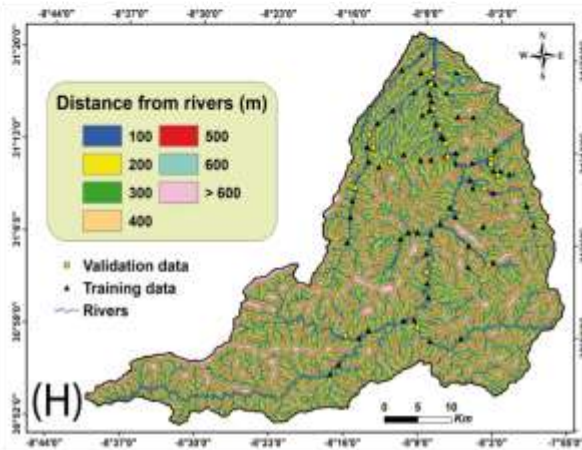
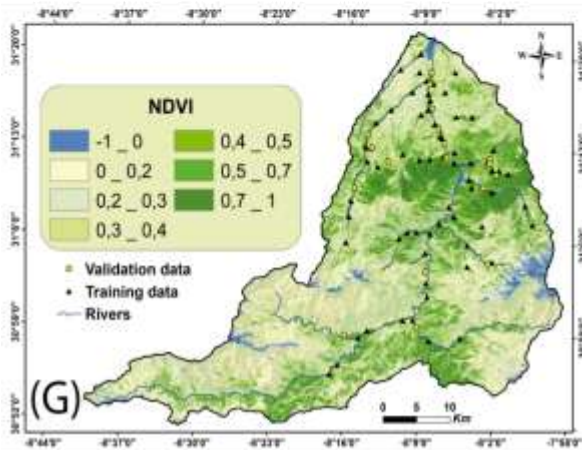
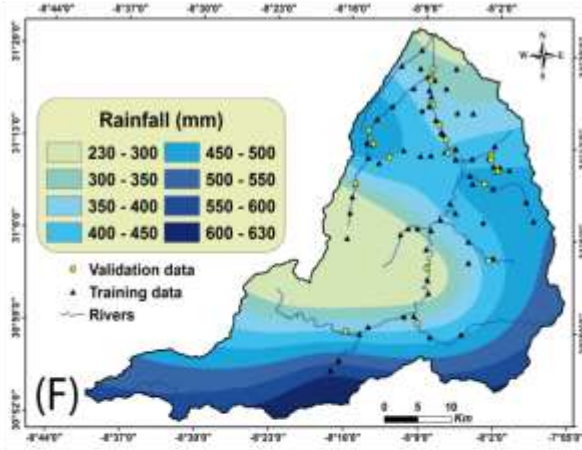
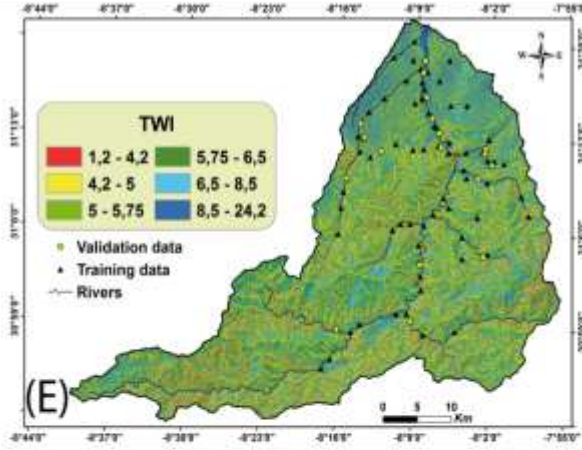
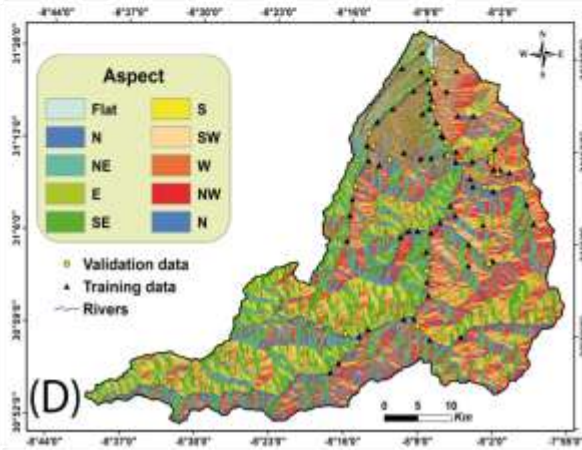
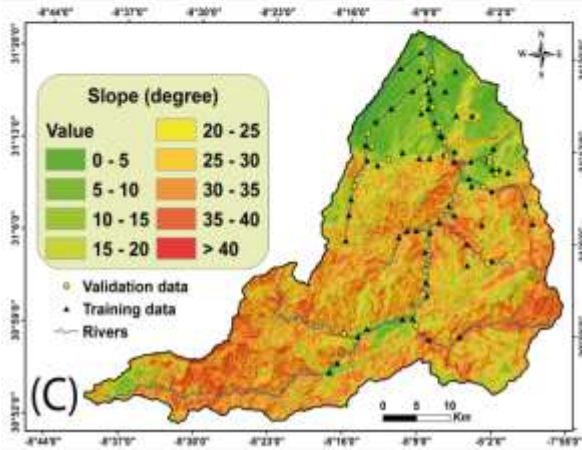
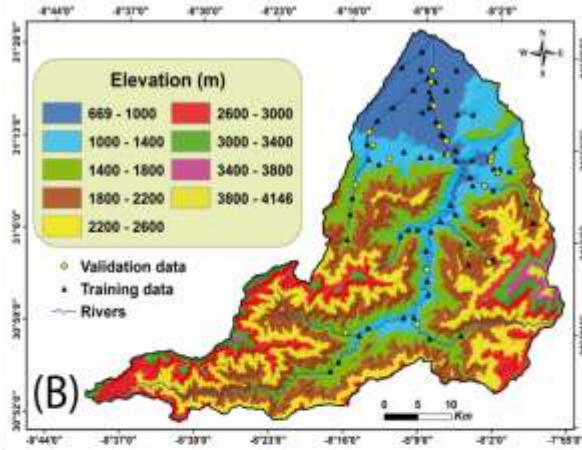
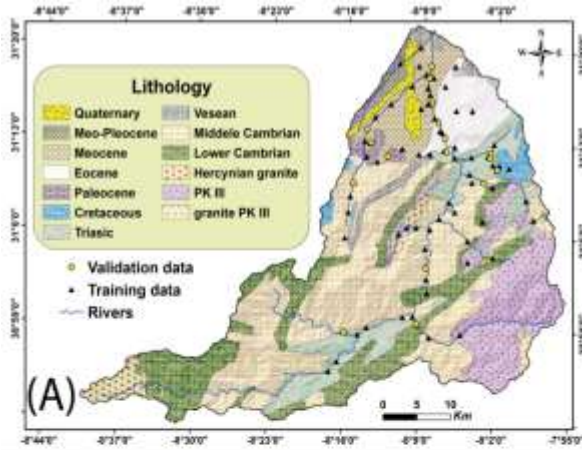
where A is the number of pixels with a flash flooding hazard for each class of each parameter; B is the total number of pixels with flash flooding hazards in study area; M is the number of pixels for each class of the parameter and N is total number of pixels in the study area. A frequency ratio value of 1 is an average value for the area flood occurring in the total area. A frequency ratio value less than 1 indicating a lower probability of flood occurrence and a value greater than 1 indicates a higher probability of flood occurrence. The FR of all the thematic layers used in the present study was calculated in GIS software and Microsoft Excel and the result is given in table 2.

Information value: The IV model is a very useful concept for the selection of variables during the construction of the model.¹⁰ In this method, the weight of the factor class is defined as the natural logarithm of the flood point density in the class divided by the flood density in the total area. The formula for IV is presented below in equation (3):²³

$$S_{if} = \ln \left(\frac{D_{if}}{D} \right) = \ln \left[\left(\frac{N_{if}}{P_{if}} \right) / \left(\frac{N}{P} \right) \right] \quad (3)$$

where S_{if} is the weight given to a given class i of the factor f , D_{if} is the flood density inside the class i of the factor f , D is the flood density inside the total area, N_{if} is the number of floods in a given class i of the parameter f , P_{if} is the number of pixels in class i of the factor f , N is the total flood within the study area and P is the total pixels inside the study area.

To apply informational value modeling, the weights of each class for all parameters were calculated in GIS software and Microsoft Excel, table 1 shows the results. The higher is the resulting weight, the more likely it is that flooding will occur in the area covered by the considered class.



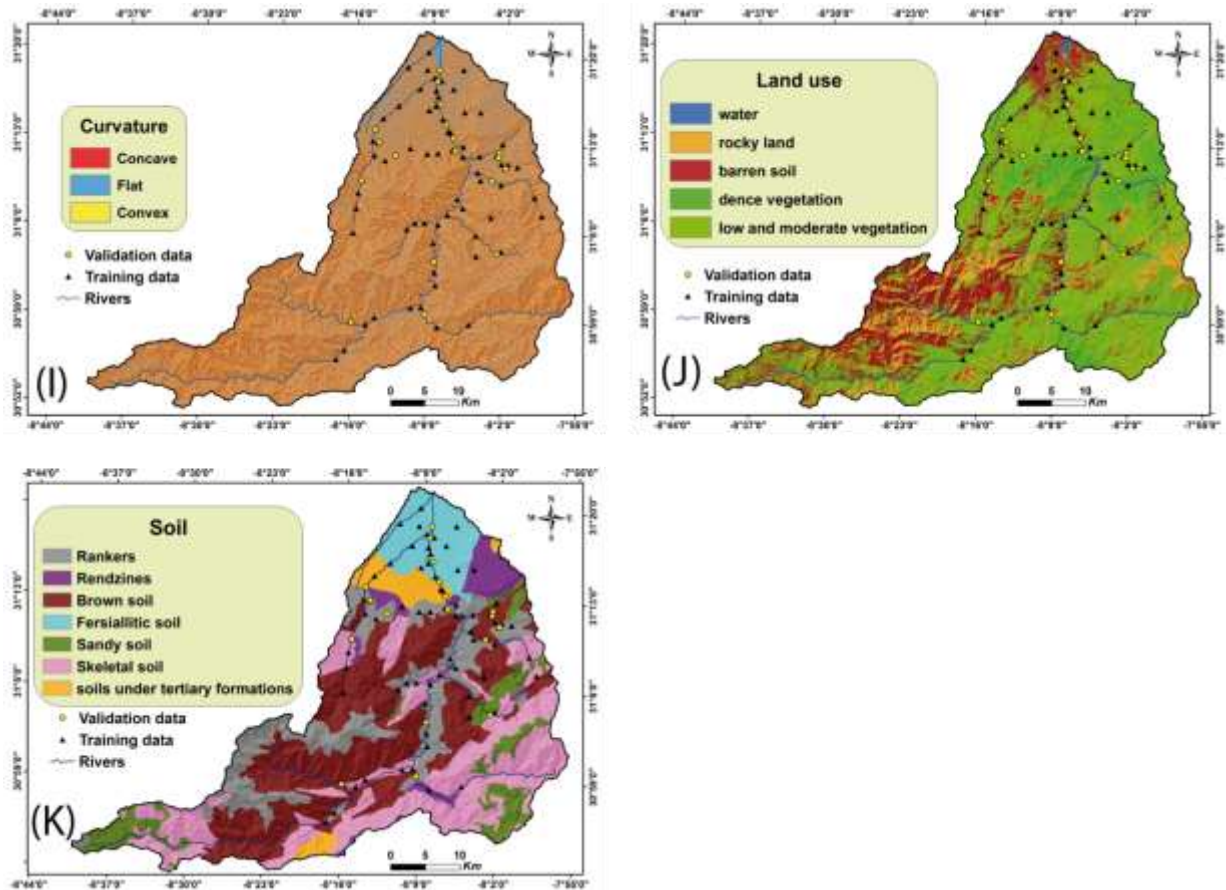


Fig. 4: Flood conditioning factor (A) lithology, (B) elevation, (C) slope, (D) aspect, (E) TWI, (F) rainfall, (G) NDVI (H) Distance to rivers, (I)curvature (J) land use and (K) soil type

Weights of evidence (WOE): Many studies have used WoE for flood susceptibility mapping.^{27,30} The Weights of Evidence belongs to bivariate statistical methods based on Bayesian probability model. The first application of this method by Bonham-Carter⁷ and et al⁶ was followed by many landslide susceptibility studies^{27,35} and also by flood susceptibility studies.^{18,34,44,45} In this data-driven method, the weights are extracted based on the analysis of the spatial relation between the flood event locations and each flood conditioning factor.^{44,45}

When performing the WOE method, two basic parameters of positive weight (W^+) and negative weight (W^-) are calculated. The weight of each flood conditioning factor (B) is obtained based on the presence or absence of the flood event location (A) in the study area⁷ using equation (4) and equation (5):

$$W^+ = \ln \frac{P\{B/A\}}{P\{B/\bar{A}\}} \quad (4)$$

$$W^- = \ln \frac{P\{\bar{B}/A\}}{P\{\bar{B}/\bar{A}\}} \quad (5)$$

where W^+ is the positive weight, W^- is the negative weight, P is the probability and \ln is the natural logarithm. B is the presence of the flood conditioning factor while \bar{B} is the absence of the flood conditioning factor. A is the presence of flood event location while \bar{A} is the absence of flood event

location.⁵⁰ In this sense, a positive weight means the existence of flood conditioning factor at the flood event locations while its magnitude defines the positive spatial relationship between these two inputs. On the other hand, negative weight means the absence of the flood conditioning factor at the flood event locations and thus negative spatial relationship.

Moreover, the difference between W^+ and W^- is described as the weight contrast (C), which can be positive for positive spatial relationship between the flood conditioning factor and flood event location or negative for negative spatial relationship.^{44,45} The weight contrast was calculated using equation (6):⁷

$$C = W^+ - W^- \quad (6)$$

Where C is the weight contrast, W^+ is the positive weight and W^- is the negative weight. The standard deviation of W was calculated with equation (7):⁷

$$S(C) = \sqrt{S^2W^+ - S^2W^-} \quad (7)$$

where $S(C)$ is the standard deviation, S^2W^+ is the variance of positive weights while S^2W^- is the variance of negative weights. The positive and negative variance of weights were calculated using equation (8) and equation (9):⁷

Table 1
Calculate weights for different classes of each factor based on the occurrences of flood

Factor	Class	Number of pixels in class	Percentage of domain (PD)	Number of flood points	Percentage of flood (PL)	F R	I V	W O E
Elevation	669 - 1000	1272189	11,61	23	33,33	2,87	5,66	0,59
	1000 - 1400	1456731	13,29	33	47,83	3,60	5,76	0,79
	1400 - 1800	1969797	17,98	9	13,04	0,73	5,06	-0,16
	1800 - 2200	2492537	22,75	4	5,80	0,25	4,61	-0,67
	2200 - 2600	1904152	17,38	0	0,00	0,00	0,00	-0,08
	2600 - 3000	1283162	11,71	0	0,00	0,00	0,00	-0,05
	3000 - 3400	411264	3,75	0	0,00	0,00	0,00	-0,02
	3400 - 3800	128853	1,18	0	0,00	0,00	0,00	-0,01
3800 -4146	39502	0,36	0	0,00	0,00	0,00	0,00	
Aspect	Flat	238676	2,18	3	4,35	2,00	5,50	0,32
	North	1394729	12,73	5	20,29	3,22	5,57	0,41
	Northeast	1311145	11,96	15	21,74	1,82	5,46	0,32
	East	1142489	10,43	1	1,45	0,14	4,34	-0,89
	Southeast	1374238	12,54	1	1,45	0,12	4,26	-0,98
	South	1270892	11,60	1	1,45	0,12	4,30	-0,94
	Southwest	1249359	11,40	3	4,35	0,38	4,78	-0,45
	West	1363696	12,44	14	20,29	1,63	5,41	0,26
Northwest	1612963	14,72	17	24,64	1,67	5,42	0,29	
Slope	0 - 5	877640	8,01	25	23,84	4,70	5,87	0,43
	5 - 10	949345	8,66	18	18,84	2,68	5,63	0,40
	10 - 15	924563	8,44	10	10,14	2,06	5,52	0,10
	15 - 20	1223898	11,17	8	11,59	1,17	5,27	0,03
	20 - 25	1521999	13,89	5	7,25	0,63	5,00	-0,31
	25 - 30	1908976	17,42	0	0,00	0,00	0,00	-0,26
	30 - 35	1750461	15,97	0	0,00	0,00	0,00	-0,04
	35 - 40	1108049	10,11	0	0,00	0,00	0,00	-0,39
40 - 80	693256	6,33	0	0,00	0,00	0,00	-0,17	
Distance to Stream	0 - 100	3038244	27,73	69	100,00	3,61	5,76	0,56
	100 - 200	2629077	23,99	0	0,00	0,00	0,00	0,00
	200 - 300	2067878	18,87	0	0,00	0,00	0,00	0,00
	300 - 400	1480579	13,51	0	0,00	0,00	0,00	0,00
	400 - 500	930448	8,49	0	0,00	0,00	0,00	0,00
	500 - 600	494119	4,51	0	0,00	0,00	0,00	0,00
	> 600	317842	2,90	0	0,00	0,00	0,00	0,00
NDVI	-1,00	308723	2,82	0	0,00	0,00	0,00	-0,01
	0 - 0,2	3585799	32,72	6	8,70	0,27	4,63	-0,70
	0,2 - 0,3	2497976	22,80	9	13,04	0,57	4,96	-0,29
	0,3 - 0,4	1397659	12,75	15	21,74	1,70	5,43	0,29
	0,4 - 0,5	903324	8,24	12	17,39	2,11	5,53	0,38
	0,5 - 0,7	1241592	11,33	13	18,84	1,66	5,42	0,27
0,7 - 1	1023114	9,34	14	20,29	2,17	5,54	0,40	
curvature	convex	2777331	25,345	7	10,145	0,40	4,803	-0,47
	Concave	3706408	33,823	36	52,174	1,54	5,389	0,34
	flat	4474448	40,832	26	37,681	0,92	5,166	-0,05
Lithology	Hercynian granite	291252	2,66	0	0,00	0,00	0,00	0,00
	Lower Cambrian	1805221	16,47	4	5,80	0,35	4,75	-0,50
	Granite PK III	161417	1,47	0	0,00	0,00	0,00	-0,01
	PK III	1487143	13,57	2	2,90	0,21	4,53	-0,71
	Triassic	1184184	10,81	17	24,64	2,28	5,56	0,44

	Middele Cambrian	3899874	35,59	16	23,19	0,65	5,01	-0,25
	Visean	205846	1,88	1	1,45	0,77	5,09	-0,11
	Paleocene	147493	1,35	1	1,45	1,08	5,23	0,04
	Cretaceous	174341	1,59	4	5,80	3,64	5,76	0,59
	Eocene	663642	6,06	9	13,04	2,15	5,53	0,37
	Miocene- pleocene	66174	7,60	15	21,45	4,94	5,98	0,89
	Quaternary	194812	1,78	0	0,00	0,00	0,00	-0,01
TP I	-97 - -15	171619	1,57	1	1,45	0,93	5,17	-0,03
	-15 - -7	1205423	11,00	6	8,70	0,79	5,10	-0,11
	-7 - -3	1723329	15,73	9	13,04	0,83	5,12	-0,09
	-3 - 1	3223516	29,42	24	34,78	1,18	5,27	0,12
	1 - 6	2931384	26,75	15	21,74	0,81	5,11	-0,11
	6 - 12	1320244	12,05	8	11,59	0,96	5,18	-0,01
	12 - 104	382672	3,49	6	8,70	2,49	5,60	0,43
soil	rankers	1875895	17,12	8	11,59	0,68	5,03	-0,19
	rendzines	498491	4,55	9	13,04	2,87	5,66	0,51
	Brown soil	3526990	32,19	17	24,64	0,77	5,08	-0,15
	fersialitic soil	892431	8,14	19	27,54	3,38	5,73	0,64
	sandy soil	879257	8,02	14	20,29	2,53	5,60	0,47
	skeletal soil	2839452	25,91	1	1,45	0,06	3,95	-1,37
	soil on tertiary formations	445671	4,07	1	1,45	0,36	4,75	-0,45
TWI	< 4,20	582243	5,31	6	8,70	0,64	5,01	0,04
	4,2 _ 5	2333240	21,29	9	13,04	0,61	4,99	-0,25
	5 _ 5,75	2904133	26,50	14	20,29	0,77	5,08	-0,14
	5,75 _ 6,5	2027508	18,50	12	17,39	0,94	5,17	-0,03
	6,5 _ 8,5	1958107	17,87	10	14,49	0,81	5,11	-0,10
	8,5 <	1152956	10,52	18	26,09	2,48	5,60	0,49
land use	water	24042	0,22	0	0,00	0,00	0,00	0,00
	dense vegetation	1964037	17,92	17	24,64	1,37	5,34	0,18
	medium to low	5461797	49,84	37	53,62	1,08	5,23	0,08
	stony ground	1326975	12,11	6	8,70	0,72	5,06	-0,15
	bare earth	2181336	19,91	9	13,04	0,66	5,02	-0,21
precipitations	< 300	569470	5,20	8	11,59	2,23	5,55	0,39
	300 - 350	1222198	11,15	9	13,04	1,17	5,27	0,08
	350 - 400	2418710	22,07	17	24,64	1,12	5,25	0,07
	400 - 450	2771891	25,30	19	27,54	1,09	5,24	0,06
	450 - 500	984840	8,99	14	20,29	2,26	5,55	0,42
	500 - 550	447141	4,08	1	1,45	0,36	4,75	-0,45
	550 - 600	775859	7,08	1	1,45	0,20	4,51	-0,71
	600<	1768078	16,13	0	0,00	0,00	0,00	-0,08

$$S^2W^+ = \frac{1}{N\{B \cap A\}} + \frac{1}{N\{\bar{B} \cap A\}} \quad (8)$$

$$S^2W^- = \frac{1}{N\{\bar{B} \cap A\}} + \frac{1}{N\{B \cap A\}} \quad (9)$$

where N is the number of unit cells. The final weight (W_{final}) is the ratio of the weight contrast (C) divided by its standard deviation $S(C)$ using equation (10):^{7,18}

$$W = \frac{C}{S(C)} \quad (10)$$

Every parameter map is crossed with the flood inventory map based on the WOE model using the GIS software and the density of the flood in each class is calculated. The

resultant weights for each thematic map for the WOE model are given in table 1.

Results and Discussion

Flood susceptibility mapping: Flood susceptibility mapping is an effective tool to prevent and control future floods event. We present below the results of the spatial prevention of vulnerability to flooding using the three models: FR; IV and WOE models (table 1).

These weights obtained after a series of analyses were assigned to their classes for each factor. Using the weighted sum option in the spatial analysis tools of ArcGIS 10.4.1, we were able to produce the final maps according to the three models.

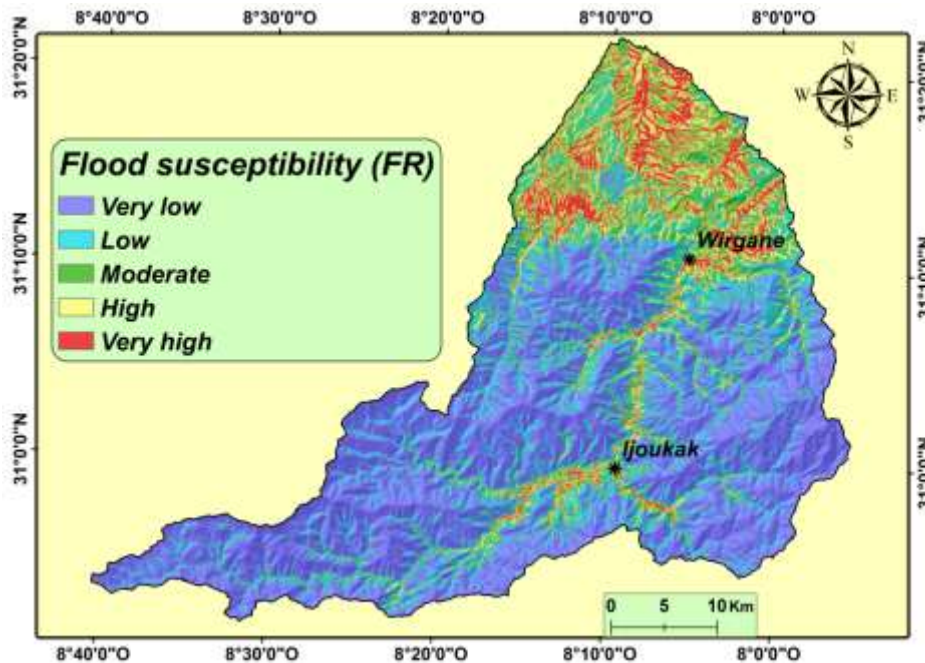


Fig. 5: Flood vulnerability mapping using the FR model.

Figures 5, 6 and 7 illustrate the flood susceptibility maps using the FR, IV and WoE models respectively after reclassifying them into five risk levels using the natural break method in ArcGIS software.

In this study, the Flood Sensitivity Index (FsI) was classified into five classes (very low, low, moderate, high and very high) using the natural break method in order to produce vulnerability maps. These maps show that areas of high to very high vulnerability are located near rivers in the southern part of the N'fis watershed as well as in the Ijoukak region in the central part of the basin. To benefit from water resources, the inhabitants settle and build houses close to the rivers, thus their property is exposed to the risk of flooding. These areas of high sensitivity represent 15.80%, 18.70% and 16.36% of the total surface area of the basin respectively according to the FR, IV and WoE model.

The resulting FR, IV and WoE susceptibility maps show close similarities between overall these three methods. The conditioning factors were classified into classes and weights are presented in columns 7, 8 and 9 of table 1. The discussion will focus on two main points: (1) Floods conditioning factors importance and (2) Validation and comparison.

Lithology is an important conditioning parameter in flooding because it has a direct influence on land permeability and thus surface runoff.¹⁶ The highest values obtained for this parameter are recorded for Triassic and Tertiary lands throughout the Cretaceous (Table 1). This can be explained by the brittleness of these formations which allows the development and branching of the hydrographic network which channels more water during episodes of heavy rainfall and as soon as this water reaches flat areas, it overflows giving rise to floods. The altitude analysis results indicate

that the lowest classes of 669–1400 m were most influential while the highest classes of 2200–4146 m were least influential on flooding (Table 1). This reflects the natural characteristics of flooding which occurs mostly in vast areas of low elevation and not on mountain peaks.

The slopes aspect has an impact on the amount of rainfall and the level of sunshine.¹ Referring to the results of table 1, it can be seen that flat lands and those oriented from north to west are the most vulnerable. The slope factor in this study shows a strong correlation between flooding and low-lying flat areas. FR ratios greater than 1 indicates that flooding occurs mainly in areas with a slope between 0° and 15°. It can therefore be deduced that the steeper is the slope, the more floods will occur in the lower parts of the catchment area (Table 1).

TWI represents the effect of topography on the location and size of saturated source zones in runoff production.⁴⁰ There is a direct relation between this parameter (soil moisture status) and the occurrence of flooding. Indeed, according to table 1, flood sensitivity increases with increasing TWI values. Precipitation is the most triggering factor in the generation of floods and without it, no floods will be generated. The highest ratio for the precipitation conditioning factor occurred in areas where there was less than 500 mm of precipitation in the south of the N'fis catchment area.

Vegetation can reduce the rate of infiltration to the ground,²¹ thus contributing to the formation of floods. Table 1 shows that the susceptibility to flooding increases as the vegetation index increases. While when vegetation is weak or absent, as in the case of bare and rocky soils, water flow is easier, thus avoiding flooding.

Soil type has a direct impact on water storage, permeability and drainage. Therefore, this factor was also taken into account in our analysis. The highest ratio was indicated by the fertile soil type with an FR ratio of 3.38 while skeletal soils had a weak relationship with the occurrence of flooding (Table 1).

One of the most important factors in flood vulnerability mapping is the distance from the river. River levels will rise due to heavier rainfall during floods, causing overflow in the areas closest to the banks. In our case, floods mainly occur and concentrate in areas within 100 meters length from the river bed. Finally, for the curvature factor, flooding occurred mainly in areas with flat surface which is confirmed by the results obtained in the study area (Table 1). This can be explained by the fact that flat terrain is more favourable likely for flooding.

Validation and comparison: Success and prediction rate curves under receiving operating characteristics (ROC) were used for assessing the overall accuracy of the training and testing data sets.

ROC curves were used to validate and compare the results of the FR, IV and WoE models. All pixels of the susceptibility classes were arranged in descending order to obtain their relative ranks. The percentage of flood susceptibility index rank was plotted on the x-axis and cumulative percentage of flood pixels on the y-axis. The area under curve (AUC) value of the success rate curves was

highest in the WoE model (88,40%) followed by the IV model (87,75%) and FR model (85,65%) (Fig. 8A). The probability of future flood occurrence was determined by the prediction rate curve. AUC value of prediction rate curves was also highest in the WoE model (87,08%) followed by the IV (86,66%) and FR (85,55%) models (Fig. 8B).

Thus, it can be concluded that the Weight of Evidence model performed better than the frequency ratio and informative value models. However, all models are effective in predicting floods vulnerability because AUC in the prediction rate curve is comparable with that in the success rate curve.

Conclusion

Generally, floods are unpredictable phenomena; however, the spatial assessment of susceptibility to flooding can be determined using various GIS-based models. In the present research, the Frequency Ratio (FR), Informative Value (IV) and Weight of Evidence (WOE) models were applied to predict the susceptibility of flood risk in the N'fis catchment area. These statistical methods were applied to establish the correlation between the conditioning factors and flood hazard. The first step was dedicated to the realization of an inventory of ancient floods in this sector by the treatment of satellite images and field missions to detect these floods sites. Subsequently, thematic maps of eleven causative factors were prepared based on several data sources.

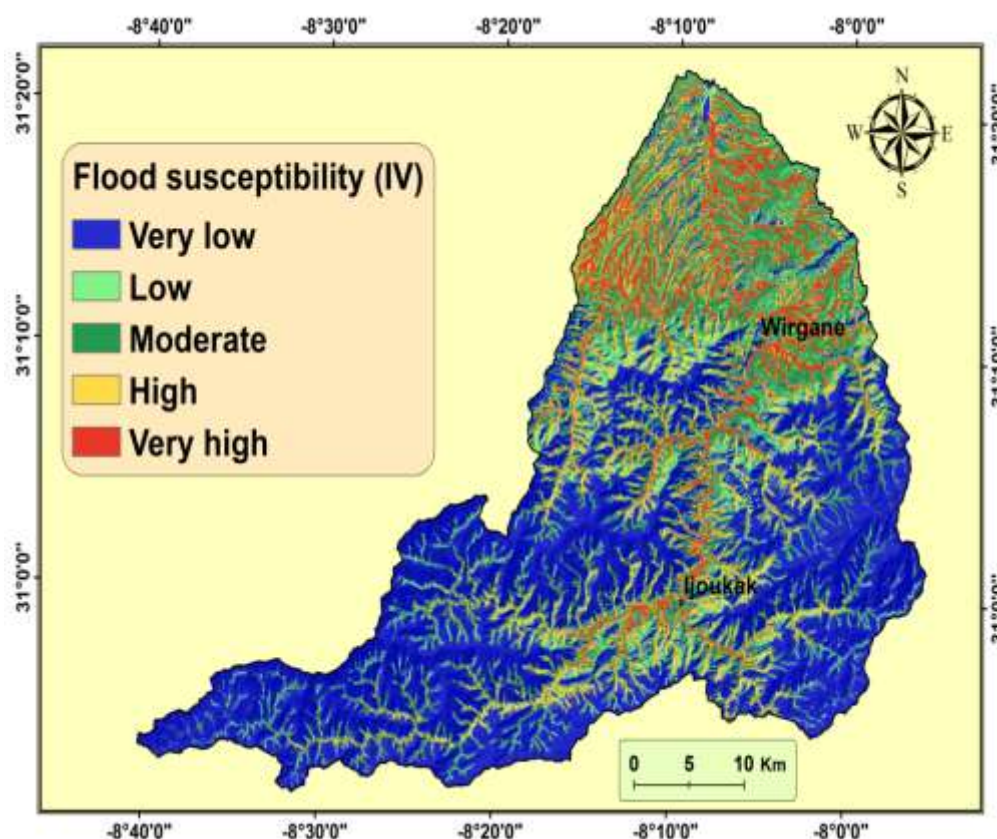


Fig. 6: Flood vulnerability mapping using the IVmodel

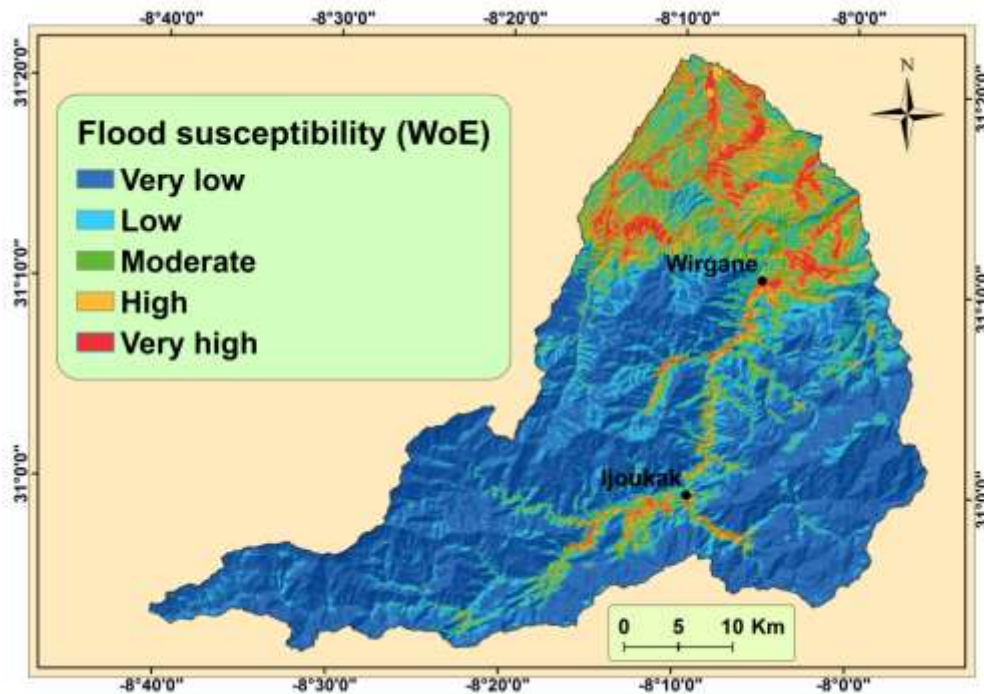


Fig. 4: Flood vulnerability mapping using the WoE model

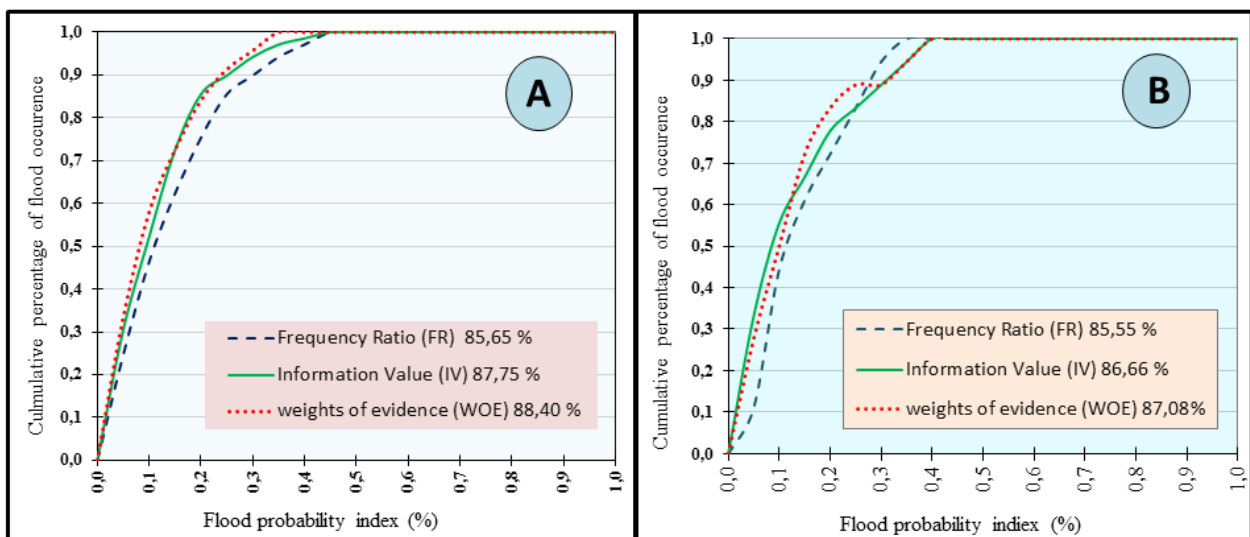


Fig. 5: ROC curves of the three models. (A) using the training dataset, (B) using the validation dataset.

Flood risk susceptibility maps obtained from the application of the three models FR, IV and WoE show that the southern regions of the basin are more vulnerable as well as the central part crossed by the main N'fis river. These regions constitute a transition zone between the high chain and the Haouz plain with moderate slopes. This shows the major effect of topography on flow processes and thus on the occurrence of floods. These regions, because of their location in the downstream part, are also affected by a large part of the rainfall received by the N'fis watershed which amplifies the risk.

Evaluation of the quality of the models applied in this research using the ROC method shows that all three models produced good quality results. The WoE model is the best

performing model followed by IV and finally FR. The sensitivity maps produced by these models can help decision-makers and planners to implement appropriate management plans in the N'fis catchment area and to confine development processes by delineating areas sensitive to flood risk.

References

1. Abubakar T., Azra E. and Mohammed C., Selecting suitable drainage pattern to minimize flooding in Sangere village using GIS and remote sensing, *Global J Geol Sci.*, **10**, 129–140 (2012)
2. Alifriqui M., M'hirit O., Michalet R. and Peltier J.P., Variabilité des précipitations dans le Haut Atlas Occidental marocain, *Le Climat*, **13**(1), 11-28 (1995)

3. Amaya A., Algouti A., Algouti A. and El Aaggad N., Cartographie de l'aléa mouvements de terrain du bassin versant de N'fis, Haut Atlas, Maroc [Mapping of mass movements hazard in the N'fis watershed, High Atlas, Morocco], *Int. J. Innov. Appl. Manag.*, **8(2)**, 64 (2014)
4. Arabameri A., Saha S., Chen W., Roy J., Pradhan B. and Bui D.T., Flash flood susceptibility modelling using functional tree and hybrid ensemble techniques, *J. Hydrol.*, **587**, 125007 (2020)
5. Benito G., Rico M., Sánchez-Moya Y., Sopena A., Thorndycraft V.R. and Barriendos M., The impact of late Holocene climatic variability and land use change on the flood hydrology of the Guadalentín River, southeast Spain, *Glob Planet Change*, **70(1-4)**, 53-63 (2010)
6. Bonham-Carter G.F., Agterberg F.P. and Wright D.F., Integration of geological datasets for gold exploration in Nova Scotia, *Photogramm Eng Remote Sensing*, **54(11)**, 1585-1592 (1988)
7. Bonham-Carter G.F., Integration of geoscientific data using GIS, *Geographic information systems: principle and applications*, Longdom, London, 171-184 (1991)
8. Bui D.T., Pradhan B., Nampak H., Bui Q.T., Tran Q.A. and Nguyen Q.P., Hybrid artificial intelligence approach based on neural fuzzy inference model and metaheuristic optimization for flood susceptibility modeling in a high-frequency tropical cyclone area using GIS, *J. Hydrol.*, **540**, 317-330 (2016)
9. Cao C., Xu P., Wang Y., Chen J., Zheng L. and Niu C., Flash flood hazard susceptibility mapping using frequency ratio and statistical index methods in coalmine subsidence areas, *Sustainability*, **8(9)**, 948 (2016)
10. Cevik E. and Topal T., GIS-based landslide susceptibility mapping for a problematic segment of the natural gas pipeline, Hendek (Turkey), *Environ. Geol.*, **44(8)**, 949-962 (2003)
11. Chowdhuri I., Pal S.C. and Chakraborty R., Flood susceptibility mapping by ensemble evidential belief function and binomial logistic regression model on river basin of eastern India, *Adv. Space Res.*, **65(5)**, 1466-1489 (2020)
12. Costache R., Pham Q.B., Avand M., Linh N.T.T., Vojtek M., Vojteková J. and Dung T.D., Novel hybrid models between bivariate statistics, artificial neural networks and boosting algorithms for flood susceptibility assessment, *J. Environ. Manage.*, **265**, 110485 (2020)
13. Diakakis M., Mavroulis S. and Deligiannakis G., Floods in Greece, a statistical and spatial approach, *Nat Hazards (Dordr)*, **62(2)**, 485-500 (2012)
14. Ercanoglu M. and Gokceoglu C., Assessment of landslide susceptibility for a landslide-prone area (north of Yenice, NW Turkey) by fuzzy approach, *Environ. Geol.*, **41(6)**, 720-730 (2002)
15. García-Ruiz J.M., Regüés D., Alvera B., Lana-Renault N., Serrano-Muela P., Nadal-Romero E. and Arnáez J., Flood generation and sediment transport in experimental catchments affected by land use changes in the central Pyrenees, *J. Hydrol.*, **356(1-2)**, 245-260 (2008)
16. Haghizadeh A., Siahkamari S., Haghiahi A.H. and Rahmati O., Forecasting flood-prone areas using Shannon's entropy model, *J Earth Syst Sci*, <https://doi.org/10.1007/s1204-0-017-0819-x>, **126**, 39 (2017)
17. Hong H., Tsangaratos P., Iliá I., Liu J., Zhu A.X. and Chen W., Application of fuzzy weight of evidence and data mining techniques in construction of flood susceptibility map of Poyang County, China, *Science of the Total Environment*, **625**, 575-588 (2018)
18. Khosravi K., Nohani E., Maroufinia E. and Pourghasemi H.R., A GIS-based flood susceptibility assessment and its mapping in Iran: a comparison between frequency ratio and weights-of-evidence bivariate statistical models with multi-criteria decision-making technique, *Nat Hazards (Dordr)*, **83(2)**, 947-987 (2016)
19. Kwak Y. and Kondoh A., A study on the extraction of multi-factor influencing floods from RS image and GIS data; a case study in Nackdong Basin, S. Korea, In *The International Archives of The Photogrammetry, Remote Sensing And Spatial Information Sciences*, ISPRS Congress Beijing, 421-426 (2008)
20. Lee M.J., Kang J.E. and Jeon S., Application of frequency ratio model and validation for predictive flooded area susceptibility mapping using GIS, In *2012 IEEE Geosci. Remote Sens. Lett.*, 895-898 (2012)
21. Lei H., Yang D. and Huang M., Impacts of climate change and vegetation dynamics on runoff in the mountainous region of the Haihe River basin in the past five decades, *J Hydrol.*, **511**, 786-799 (2014)
22. Liao X. and Carin L., Migratory logistic regression for learning concept drift between two data sets with application to UXO sensing, *IEEE Trans Geosci Remote Sens*, **47(5)**, 1454-1466 (2009)
23. Manchar N., Benabbas C., Hadji R., Bouaicha F. and Grecu F., Landslide susceptibility assessment in Constantine region (NE Algeria) by means of statistical models, *Studia Geotech. et Mech.*, **40(3)**, 208-219 (2018)
24. Mathieu P., Caractérisation des sols et de leurs propriétés hydrodynamiques pour la modélisation hydrologique en milieu semi-aride, Bassin versant du Tensift-Maroc, Mémoire de fin d'étude ENSAM DAA « Physique des surfaces naturelles et géniehydrologique » (ENSAR) Avril 2002-Septembre (2002)
25. Merz B., Thielen A.H. and Gocht M., Flood risk mapping at the local scale: concepts and challenges, *Flood Risk Manag.*, 231-251 (2007)
26. Miller J.R., Morphometric assessment of lithologic controls on drainage basin evolution in the Crawford upland, south-central Indiana, Miller Jerry R., Ritter Dale F.* and Craig Kochel R., *Am. J. Sci.*, **290**, 569-599 (1990)
27. Mohammady M., Pourghasemi H.R. and Pradhan B., Landslide susceptibility mapping at Golestan Province, Iran: a comparison between frequency ratio, Dempster-Shafer and weights-of-evidence models, *J Asian Earth Sci*, **61**, 221-236 (2012)
28. Nahid A. and Benzakour M., Enregistrements sédimentaires et contrôle tectonique dans la genèse des archives

- morphosedimentaires quaternaires de la coupe d'alhnayn (Vallée Meridienne Du N'fis, Maroc), *Estud. Geol.*, **58(5-6)**, 145-158 (2002)
29. Pham B.T., Avand M., Janizadeh S., Phong T.V., Al-Ansari N., Ho L.S. and Jafari F., GIS based hybrid computational approaches for flash flood susceptibility assessment, *Water*, **12(3)**, 683 (2020)
30. Pourghasemi H.R., Pradhan B., Gokceoglu C., Mohammadi M. and Moradi H.R., Application of weights-of-evidence and certainty factor models and their comparison in landslide susceptibility mapping at Haraz watershed, Iran, *Arab. J. Geosci.*, **6(7)**, 2351-2365 (2013)
31. Pradhan B., Flood susceptible mapping and risk area delineation using logistic regression, GIS and remote sensing, *J. Spat. Hydrol.*, **9(2)**, 1-18 (2010)
32. Pradhan B., Abokharima M.H., Jebur M.N. and Tehrany M.S., Land subsidence susceptibility mapping at Kinta Valley (Malaysia) using the evidential belief function model in GIS, *Natural Hazards*, **73(2)**, 1019-1042 (2014)
33. Rahmati O., Zeinivand H. and Besharat M., Flood hazard zoning in Yasooj region, Iran, using GIS and multi-criteria decision analysis, *Geomat Nat Hazard Risk*, <https://doi.org/10.1080/19475705.2015.1045043> (2016)
34. Rahmati O., Pourghasemi H.R. and Zeinivand H., Flood susceptibility mapping using frequency ratio and weights-of-evidence models in the Golastan Province, Iran, *Geocarto Int*, **31(1)**, 42-70 (2016)
35. Regmi A.D., Devkota K.C., Yoshida K., Pradhan B., Pourghasemi H.R., Kumamoto T. and Akgun A., Application of frequency ratio, statistical index and weights-of-evidence models and their comparison in landslide susceptibility mapping in Central Nepal Himalaya, *Arab. J. Geosci.*, **7(2)**, 725-742 (2014)
36. Rifai N., Khattabi A. and Rhazi L., Modélisation des crues des rivières pour la gestion intégrée du risque d'inondation: cas du bassin versant de Tahaddart (nord-ouest du Maroc), *Revue des Sciences de l'eau/Journal of Water Science*, **27(1)**, 57-69 (2014)
37. Sahana M., Rehman S., Sajjad H. and Hong H., Exploring effectiveness of frequency ratio and support vector machine models in storm surge flood susceptibility assessment: A study of Sundarban Biosphere Reserve, India, *Catena*, **189**, 104450 (2020)
38. Salvati P., Bianchi C., Rossi M. and Guzzetti F., Societal landslide and flood risk in Italy, *Nat. Hazards Earth Syst. Sci.*, **10(3)**, 465-483 (2010)
39. Samanta S., Pal D.K. and Palsamanta B., Flood susceptibility analysis through remote sensing, GIS and frequency ratio model, *Applied Water Science*, **8(2)**, 66 (2018)
40. Sharif H.O., Al-Juaidi F.H., Al-Othman A., Al-Dousary I., Fadda E., Jamal-Uddeen S. and Elhassan A., Flood hazards in an urbanizing watershed in Riyadh, Saudi Arabia, *Geomat Nat Hazards Risk*, **7**, 702-720 (2016)
41. Simona N. and Cedric L., Gestion durable des zones inondables dans le Delta du Danube (Roumanie), 1 Journées Scientifiques Inter-Réseaux de l'AUF, Gestion Intégrée des Eaux et des Sols, Ressources, Aménagements et Risques en Milieux Ruraux et Urbains, 6-9 (2007)
42. Smith K. and Ward R., Mitigating and Managing Flood Losses, Floods: Physical Processes and Human Impacts (1998)
43. Tehrany M.S., Pradhan B. and Jebur M.N., Spatial prediction of flood susceptible areas using rule based decision tree (DT) and a novel ensemble bivariate and multivariate statistical models in GIS, *J. Hydrol.*, **504**, 69-79 (2013)
44. Tehrany M.S., Pradhan B. and Jebur M.N., Flood susceptibility mapping using a novel ensemble weights-of-evidence and support vector machine models in GIS, *J. Hydrol.*, **512**, 332-343 (2014)
45. Tehrany M.S., Lee M.J., Pradhan B., Jebur M.N. and Lee S., Flood susceptibility mapping using integrated bivariate and multivariate statistical models, *Environ. Earth Sci.*, **72(10)**, 4001-4015 (2014)
46. Tehrany M.S., Pradhan B. and Jebur M.N., Flood susceptibility analysis and its verification using a novel ensemble support vector machine and frequency ratio method, *Stoch Environ Res Risk Assess*, **29(4)**, 1149-1165 (2015)
47. Tehrany M.S. and Kumar L., The application of a Dempster-Shafer-based evidential belief function in flood susceptibility mapping and comparison with frequency ratio and logistic regression methods, *Environ. Earth Sci.*, **77(13)**, 490 (2018)
48. Wilson J.P. and Gallant J.C., Eds., Terrain analysis: principles and applications, John Wiley and Sons (2000)
49. Wanders N., Karssenberg D., De Roo A., De Jong S.M. and Bierkens M.F.P., The suitability of remotely sensed soil moisture for improving operational flood forecasting, *Hydrol Earth Syst Sci.*, **10(11)**, 13783-13816 (2013)
50. Xu C., Xu X., Dai F., Xiao J., Tan X. and Yuan R., Landslide hazard mapping using GIS and weight of evidence model in Qingshui river watershed of 2008 Wenchuan earthquake struck region, *J. Earth Sci.*, **23(1)**, 97-120 (2012).

(Received 03rd June 2021, accepted 05th August 2021)